IOPscience iopscience.iop.org

Home Search Collections Journals About Contact us My IOPscience

Modeling the reactive ion etching process for the CoO(001) surface *via* first principles calculations

This article has been downloaded from IOPscience. Please scroll down to see the full text article.

2008 J. Phys.: Condens. Matter 20 355006

(http://iopscience.iop.org/0953-8984/20/35/355006)

View the table of contents for this issue, or go to the journal homepage for more

Download details:
IP Address: 129.252.86.83
The article was downloaded on 29/05/2010 at 14:40

Please note that terms and conditions apply.

IOP PUBLISHING JOURNAL OF PHYSICS: CONDENSED MATTER

J. Phys.: Condens. Matter **20** (2008) 355006 (5pp) doi:10.1088/0953-8984/20/35/355006

Modeling the reactive ion etching process for the CoO(001) surface *via* first principles calculations

Nobuki Ozawa, Tanglaw Roman, Melanie David, Hirofumi Kishi and Hideaki Kasai[1]

Division of Precision Science and Technology and Applied Physics, Osaka University, Suita, Osaka, 565-0871, Japan

E-mail: kasai@dyn.ap.eng.osaka-u.ac.jp

Received 2 May 2008, in final form 15 July 2008
Published 1 August 2008
Online at stacks.iop.org/JPhysCM/20/355006

Abstract
Using first principles calculations with local density approximation (LDA) and LDA + U methods, we present a detailed theoretical study of reactive gas combinations (O_2, N_2, CH_4, and CHF_3) for the etching processes of CoO(001) surfaces. The calculation results show that the best possible gas combinations for the etching process contain CH_4. Despite differences in the intermediate state total energies predicted by the two methods, the favorable results in the final state lead to the same reaction products.

1. Introduction

In micro-fabrication technology, reactive ion etching (RIE), which uses chemically reactive ions to fabricate surfaces [1–5], is available for etching transition metal oxide (TMO) surfaces such as CoO, NiO, and TiO_2 [6]. These metal oxides are essential materials in fabricating the components of a high capacious and nonvolatile device such as a resistive random access memory (ReRAM) [7–10], consisting of metal/TMO/metal trilayers. Here, in order to fabricate the TMO layer without residues, it is important to determine the optimum reaction gas combination. Thus, the combinations of reactive gas molecules for the RIE of TMO surfaces have been studied using several different approaches [11–14]. For instance, halogenide gas is found to be an effective etchant for semiconductor surfaces [1, 2]. Other reactive gases combined with CH_4 and H_2 have also been successfully used experimentally [3–5]. Hence, these molecules are expected to work effectively in etching TMO surfaces. For this reason, we have investigated the reaction processes via first principles calculations and attempted to suggest optimum gas combinations for the RIE of TMO surfaces [7–10]. However, it is known for a fact that there are some shortcomings in predicting the physical properties of strongly correlated systems such as CoO, NiO, and TiO_2 using local density approximation (LDA) due to the correlation effects in the localized orbitals of transition metal atoms in the TMOs [15, 16]. However, by introducing an effective Coulomb interaction U (a strong intra-atomic interaction in a Hartree–Fock like manner), these shortcomings can be removed. This theoretical technique is called the LDA + U method [17, 18]. In this study, we present our investigations on the etching process of CoO(001) using reactive gas molecules (O_2, N_2, CH_4, and CHF_3) by calculating the total energies on three elementary reaction states: (i) initial state (surface and isolated molecules), (ii) intermediate state (surface and adsorbed molecules), (iii) final state (etched surface and isolated by-products generated in etching processes). We obtain the total energy differences for each state in order to determine whether the etching process proceeds or not. We also compare the LDA and LDA + U methods and their significance in the computational material design for the etching process.

This paper is organized as follows. In the next section, we give a detailed description of the method of calculating the total energies in the different states using LDA and LDA + U approaches. In section 3, we present our discussion on the predicted gas combinations for the effective etching of the CoO(001) surface based on our calculation results. We also describe the influence of the LDA + U method in the total energies of etching processes on the CoO(001) surface. Section 4 contains a summary of this work.

[1] Author to whom any correspondence should be addressed.

 © 2008 IOP Publishing Ltd Printed in the UK

Table 1. Magnetic moments M_{Co} (μ_B per Co atom), band gaps E_g (eV), and U values (eV) used for a CoO bulk.

U (eV)	M_{Co} (μ_B)	E_g (eV)
0.0	2.330	0.543
3.0	2.529	1.179
4.0	2.598	1.607
5.0	2.659	2.053
6.0	2.713	2.239
7.0	2.759	2.585
8.0	2.804	2.763

2. Theory

The total energies in the initial, intermediate, and final states in the etching process are calculated based on density functional theory using the projector augmented wave (PAW) method [19] as implemented in the VASP code [20]. For the exchange correlation energy, we have considered the LDA and the LDA + U methods. Both methods are carried out using slabs consisting of four atomic layers in a (2 × 2) unit cell, which are repeated periodically. A vacuum with a size equivalent to six atomic layers is set between the slabs. In all calculations, an energy cutoff of 400 eV and a 9 × 9 × 1 k-point mesh are adopted for the CoO(001) surface in order to ensure that the total energies converged. In addition, the first atomic layer is relaxed since adsorbed molecules give the most influence on the first atomic layer. The lattice constant adopted for CoO(001) is 3.26 Å [21]. In performing the LDA + U approach, the appropriate U value should be determined. Table 1 shows the magnetic moment values per Co atom and the band gap values of the CoO bulk in seven different U values. When U takes a value of 7.0 eV, although the corresponding magnetic moment does not fit the experimental value [22], the corresponding band gap is in good agreement with the experimental value of 2.4 eV [23]. Thus, we have chosen U of 7.0 eV for all calculations of the total energies. The total energies in the initial state are obtained using the sum of the total energy of the isolated slab and that of isolated reactive gas molecules. Those in the intermediate state correspond to the sum of the total energy of the slab and adsorbed gas molecules. Those in the final state are defined as the sum of the total energy of the CoO(001) with a Co atom vacancy, the etched Co atom and the by-product molecules. The reaction processes are supposed to proceed when the total energy in the final state is lower than the one in the initial state. However, when the by-product gas in the final state is nonvolatile, the corresponding reaction process is not efficient. In these total energy calculations, the structures of the etching molecules and the surface are optimized in all states.

3. Results and discussions

The chemical equations in the reaction process of the reactive gas molecules on the CoO(001) surface, and the total energy differences between the initial and intermediate (final) states using the LDA and LDA + U method are given in tables 2 and 3, respectively. Here, the energy origin is set as the total energy in an initial state. As stated there, [CoO(001)–Co] refers to the CoO(001) surface with a Co atom vacancy, and [ad] indicates the adsorbed molecule on the surface. In these tables, the negative values of total energy differences between the initial and intermediate (final) states indicate that the reaction processes can proceed to the intermediate (final) states. When the same reactive gas is used in two or more reaction processes, the one with the lower total energy in the final state should be more favorable in the etching process. In addition, a positive total energy value in the intermediate state corresponds to an activation barrier in the reaction process. Although some processes have activation barriers of a few eV, these reactions can still proceed due to the applied initial thermal energy to the gas molecules during the etching process. However, a much higher activation barrier in the intermediate state disturbs the reaction process. Among all reactions which are exothermic and barrierless, the optimum process is simply that with the lowest total energy value in the final state. In addition, the reaction by-products should be volatile.

In equations (2.1)–(2.4) shown in table 2, the reactive gases contain CH_4. The by-products in equations (2.1) and (2.2) include $Co(CO)_2$, while equations (2.3) and (2.4) include $Co_2(CO)_8$. Consequently, the etching processes using CH_4 as the reactive gas can proceed since the total energies in the intermediate states and final states take negative values. Here, $Co(CO)_2$ and $Co_2(CO)_8$ are volatile. In the next sets of equations (2.5)–(2.9), the reactive gases are comprised of CHF_3, O_2, and N_2 with CoF_2, $Co(CO)_2$, and $Co_2(CO)_8$ as the by-products. Equations (2.5) and (2.6), where the reactive gas CHF_3 is combined with O_2, indicate that HF is difficult to generate when the by-product gas contains CoF_2. Although the total energies in the intermediate and final states have negative values the etching process using CHF_3 is unfavorable due to the nonvolatility of CoF_2. Using CHF_3 as the reactive gas, the by-products $Co(CO)_2$ and $Co_2(CO)_8$, even if they are volatile, are difficult to generate, as shown in equations (2.8) and (2.9). Thus, CHF_3 is an unsuitable reactive gas in etching the CoO surface.

In order to check if N_2 promotes the etching reaction as used in other metals [1], N_2 is incorporated in equations (2.2), (2.4), and (2.7). While N_2 makes the total energy values in the intermediate states somewhat low, those in the final state becomes higher. Thus, for the reactive gas containing CH_4 and CHF_3, N_2 does not promote the etching process of the CoO surface. Finally, CH_4 and CHF_3 are combined with O_2 in order to produce CoF_2, $Co(CO)_2$, and $Co_2(CO)_8$ volatile gases. The total energy in the final state with CoF_2 (2.11) as corresponding by-product is much lower than those with $Co(CO)_2$ (10) and $Co_2(CO)_8$ (2.12). However, since CoF_2 is nonvolatile the etching process for this combination is unfavorable. To summarize the above discussion, the most effective etching reaction of the CoO(001) surface can be initiated with reactive gases including CH_4 and O_2, producing $Co_2(CO)_8$ and H_2O as by-products, as shown in equation (2.3) in table 2.

In table 3, it can be observed that the total energies in all three states are lowered by about 3 eV after applying the LDA + U method, and intermediate states, when compared with the initial states, are all lower in energy. As can be

Table 2. Chemical reaction equations and total energies for the CoO(001) surface and reactive gas combinations with the LDA method. The origin is set as the total energy in an initial state.

	Initial state	Intermediate state	Final state	
CH_4	$CoO(001) + 2CH_4 + 3O_2$	$CoO(001) + 2CH_4[ad] + 3O_2[ad]$	$[CoO(001)–Co] + Co(CO)_2 + 4H_2O$	(2.1)
	0.000 (eV)	−1.016 (eV)	−5.253 (eV)	
	$CoO(001) + 2CH_4 + O_2 + 4/3N_2$	$CoO(001) + 2CH_4[ad] + O_2[ad] + 4/3N_2[ad]$	$[CoO(001)–Co] + Co(CO)_2 + 8/3NH_3$	(2.2)
	0.000 (eV)	−2.218 (eV)	−1.143 (eV)	
	$CoO(001) + 4CH_4 + 6O_2$	$CoO(001) + 4CH_4[ad] + 6O_2[ad]$	$[CoO(001)–Co] + 1/2Co_2(CO)_8 + 8H_2O$	(2.3)
	0.000 (eV)	−2.033 (eV)	−20.122 (eV)	
	$CoO(001) + 4CH_4 + 9/2O_2 + N_2$	$CoO(001) + 4CH_4[ad] + 9/2O_2[ad] + N_2[ad]$	$[CoO(001)–Co] + 1/2Co_2(CO)_8 + 5H_2O + 2NH_3$	(2.4)
	0.000 (eV)	−4.436 (eV)	−11.903 (eV)	
CHF_3	$CoO(001) + 2/3CHF_3 + 5/6O_2$	$CoO(001) + 2/3CHF_3[ad] + 5/6O_2[ad]$	$[CoO(001)–Co] + CoF_2 + 2/3CO_2 + 1/3H_2$	(2.5)
	0.000 (eV)	−0.305 (eV)	−1.837 (eV)	
	$CoO(001) + CHF_3 + O_2$	$CoO(001) + CHF_3[ad] + O_2[ad]$	$[CoO(001)–Co] + CoF_2 + CO_2 + HF$	(2.6)
	0.000 (eV)	−0.277 (eV)	−0.969 (eV)	
	$CoO(001) + 2/3CHF_3 + 2/3O_2 + 1/9N_2$	$CoO(001) + 2/3CHF_3[ad] + 2/3O_2[ad] + 1/9N_2[ad]$	$[CoO(001)–Co] + CoF_2 + 2/3CO_2 + 2/9NH_3$	(2.7)
	0.000 (eV)	−0.405 (eV)	−1.495 (eV)	
	$CoO(001) + 2CHF_3 + 3/2O_2$	$CoO(001) + 2CHF_3[ad] + 3/2O_2[ad]$	$[CoO(001)–Co] + Co(CO)_2 + H_2O + 3F_2$	(2.8)
	0.000 (eV)	−0.462 (eV)	14.209 (eV)	
	$CoO(001) + 4CHF_3 + 3O_2$	$CoO(001) + 4CHF_3[ad] + 3O_2[ad]$	$[CoO(001)–Co] + 1/2Co2(CO)_8 + 2H_2O + 6F_2$	(2.9)
	0.000 (eV)	−1.493 (eV)	18.801 (eV)	
CH_4 and CHF_3	$CoO(001) + CHF_3 + CH_4 + 3/2O_2$	$CoO(001) + CHF_3[ad] + CH_4[ad] + 3/2O_2[ad]$	$[CoO(001)–Co] + Co(CO)_2 + H_2O + 3HF$	(2.10)
	0.000 (eV)	−0.756 (eV)	17.770 (eV)	
	$CoO(001) + 2/3CHF_3 + CH_4 + 17/6O_2$	$CoO(001) + 2/3CHF_3[ad] + CH_4[ad + 17/6O_2[ad$	$[CoO(001)–Co] + CoF_2 + 5/3CO_2 + 7/3H_2O$	(2.11)
	0.000 (eV)	−0.897 (eV)	−9.529 (eV)	
	$CoO(001) + 2CHF_3 + 2CH_4 + 3O_2$	$CoO(001) + 2CHF_3[ad] + 2CH_4[ad] + 3O_2[ad]$	$[CoO(001)–Co] + 1/2Co_2(CO)_8 + 2H_2O + 6HF$	(2.12)
	0.000 (eV)	1.709 (eV)	25.923 (eV)	

seen from the results in the intermediate state, the adsorption energies of the gas molecules are lowered due to the LDA + U method. The LDA + U gives a more accurate description of the actual process since U is determined so that the calculated band gap values are in agreement with experimental data. The reaction processes calculated with the LDA + U approach also show that the optimum reactive gas consists of CH_4 and O_2, and the most probable by-product contains $Co_2(CO)_8$ (equation (3.3)). This is the same optimum combination found with the LDA method. For the reactive gas containing CHF_3, the calculated reaction processes with the LDA + U show that CoF_2 is easily generated as a by-product, but volatile carbonyls are difficult. As shown in equation (3.6), although the total energy difference between the initial and final states after applying the LDA + U method changes from a positive value to a negative value, the corresponding reaction process is unfavorable since CoF_2 is nonvolatile. By including N_2 in the reactive gas, the total energies in the intermediate and final states with the LDA + U method increase. Furthermore, when CH_4 and CHF_3 are selected as the reactive etching gas, including N_2 does not promote the corresponding reaction process as shown in equations (3.2), (3.4), and (3.7).

Table 4 gives the geometries of the substrate surface and adsorbed molecule, and the adsorption energies of the molecules on the CoO(001) surface. In comparison with the optimum structure of the substrate surface and adsorbed molecules found with the LDA and LDA + U methods, the specific distinctions of those geometries are invisible, as shown in figure 1. However, in the case of the LDA + U application, while the compression of the atomic layer and the distances between the top atomic layers and the nearest atoms of the adsorbed molecules for N_2 and O_2 are unchanged, those for CH_4 and CHF_3 are slightly changed. Moreover, the adsorption energies of CH_4 and CHF_3 become higher due to the LDA + U method. On the other hand, the adsorption energies of N_2 and O_2 are lower by about −2.2 and −1.0 eV despite having the same geometry, respectively. Thus, the total energies in the intermediate state are considerably lower in the reactive gas containing much O_2 and N_2 after the LDA + U application, although adsorbed CH_4 and CHF_3 show repulsive interactions with the CoO(001) surface. Despite the differences in the intermediate state total energies predicted by the two methods, the results in the final state lead to the same reaction products.

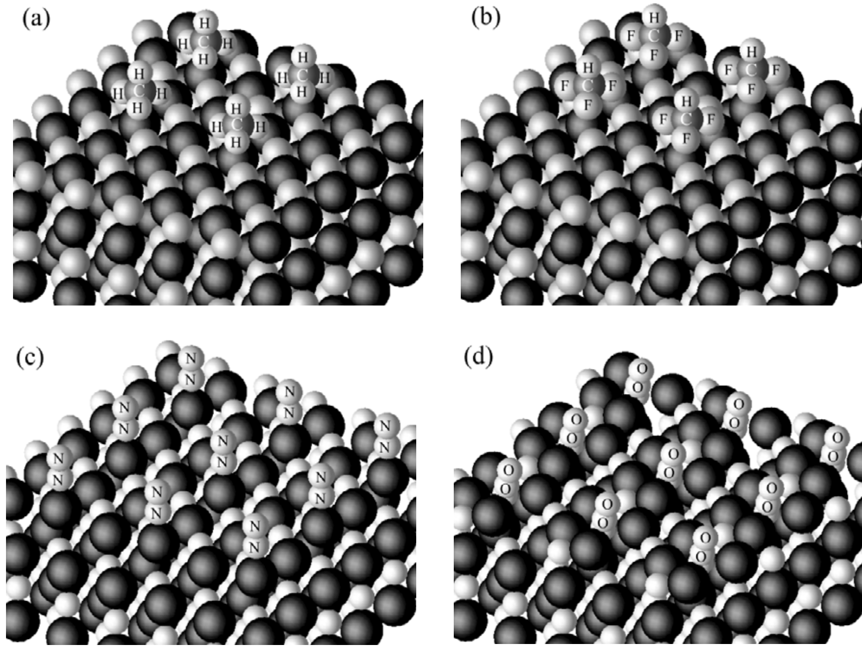

Figure 1. Optimum geometry of adsorbed molecules ((a) CH_4, (b) CHF_3, (c) N_2, (d) O_2) on the CoO(001) surface.

Table 3. The same as table 2, but for the LDA + U method.

	Initial state	Intermediate state	Final state	
CH_4	$CoO(001) + 2CH_4 + 3O_2$	$CoO(001) + 2CH_4[ad] + 3O_2[ad]$	$[CoO(001)–Co] + Co(CO)_2 + 4H_2O$	(3.1)
	0.000 (eV)	−5.106 (eV)	−7.471 (eV)	
	$CoO(001) + 2CH_4 + O_2 + 4/3N_2$	$CoO(001) + 2CH_4[ad] + O_2[ad] + 4/3N_2[ad]$	$[CoO(001)–Co] + Co(CO)_2 + 8/3NH_3$	(3.2)
	0.000 (eV)	−3.535 (eV)	−3.361 (eV)	
	$CoO(001) + 4CH_4 + 6O_2$	$CoO(001) + 4CH_4[ad] + 6O_2[ad]$	$[CoO(001)–Co] + 1/2Co_2(CO)_8 + 8H_2O$	(3.3)
	0.000 (eV)	−10.211 (eV)	−22.340 (eV)	
	$CoO(001) + 4CH_4 + 9/2O_2 + N_2$	$CoO(001) + 4CH_4[ad] + 9/2O_2[ad] + N_2[ad]$	$[CoO(001)–Co] + 1/2Co_2(CO)_8 + 5H_2O + 2NH_3$	(3.4)
	0.000 (eV)	−7.069 (eV)	−14.122 (eV)	
CHF_3	$CoO(001) + 2/3CHF_3 + 5/6O_2$	$CoO(001) + 2/3CHF_3[ad] + 5/6O_2[ad]$	$[CoO(001)–Co] + CoF_2 + 2/3CO_2 + 1/3H_2$	(3.5)
	0.000 (eV)	−1.301 (eV)	−4.055 (eV)	
	$CoO(001) + CHF_3 + O_2$	$CoO(001) + CHF_3[ad] + O_2[ad]$	$[CoO(001)–Co] + CoF_2 + CO_2 + HF$	(3.6)
	0.000 (eV)	−0.920 (eV)	−3.187 (eV)	
	$CoO(001) + 2/3CHF_3 + 2/3O_2 + 1/9N_2$	$CoO(001) + 2/3CHF_3[ad] + 2/3O_2[ad] + 1/9N_2[ad]$	$[CoO(001)–Co] + CoF_2 + 2/3CO_2 + 2/9NH_3$	(3.7)
	0.000 (eV)	−1.170 (eV)	−3.713 (eV)	
	$CoO(001) + 2CHF_3 + 3/2O_2$	$CoO(001) + 2CHF_3[ad] + 3/2O_2[ad]$	$[CoO(001)–Co] + Co(CO)_2 + H_2O + 3F_2$	(3.8)
	0.000 (eV)	−1.678 (eV)	11.991 (eV)	
	$CoO(001) + 4CHF_3 + 3O_2$	$CoO(001) + 4CHF_3[ad] + 3O_2[ad]$	$[CoO(001)–Co] + 1/2Co_2(CO)_8 + 2H_2O + 6F_2$	(3.9)
	0.000 (eV)	−3.283 (eV)	16.583 (eV)	
CH_4 and CHF_3	$CoO(001) + CHF_3 + CH_4 + 3/2O_2$	$CoO(001) + CHF_3[ad] + CH_4[ad] + 3/2O_2[ad]$	$[CoO(001)–Co] + Co(CO)_2 + H_2O + 3HF$	(3.10)
	0.000 (eV)	−1.649 (eV)	15.552 (eV)	
	$CoO(001) + 2/3CHF_3 + CH_4 + 17/6O_2$	$CoO(001) + 2/3CHF_3[ad] + CH_4[ad] + 17/6O_2[ad]$	$[CoO(001)–Co] + CoF_2 + 5/3CO_2 + 7/3H_2O$	(3.11)
	0.00 (eV)	−4.996 (eV)	−11.747 (eV)	
	$CoO(001) + 2CHF_3 + 2CH_4 + 3O_2$	$CoO(001) + 2CHF_3[ad] + 2CH_4[ad] + 3O_2[ad]$	$[CoO(001)–Co] + 1/2Co_2(CO)_8 + 2H_2O + 6HF$	(3.12)
	0.000 (eV)	−3.297 (eV)	23.705 (eV)	

Table 4. Substrate surface and adsorbed molecule distances and the adsorption energies of the molecules on the CoO(001) surface. Δd_{Co} and Δd_O indicate the change of the distance between the first and second atomic layers of Co and O atoms, respectively. A negative value corresponds to compression of the surface. d_m presents the distance between the top atomic layer and the nearest atom of the adsorbed molecule. Adsorption energy is defined as the difference between the total energy in the intermediate state and the sum of the total energy of the slab and adsorbed gas molecules.

	CH_4	CHF_3	N_2	O_2
	LDA			
Δd_{Co} (Å)	−0.16	−0.19	−0.38	−0.34
Δd_O (Å)	−0.05	−0.06	−0.33	−0.50
d_m (Å)	2.63	2.93	2.20	2.04
Adsorption energy (eV)	−0.256	−0.247	−0.168	−1.208
	LDA + U			
Δd_{Co} (Å)	−0.18	−0.17	−0.38	−0.34
Δd_O (Å)	−0.19	−0.20	−0.34	−0.51
d_m (Å)	2.77	3.07	2.17	2.04
Adsorption energy (eV)	0.874	0.904	−2.324	−2.249

In comparison with the RIE process for the NiO(001) surface [14], adding N_2 to the reactive gas mixture makes the etching process more favorable. This feature is not observed in the etching process for CoO(001).

Although this paper only provides an initial study regarding the etching of a TMO surface, the computational model design that has been used for the previous and present studies is expected to be very useful in determining favorable gas combinations and the probable by-products for an effective RIE process. Moreover, by experimental methods such as mass spectrometry [24], the actual by-products must be confirmed. If a disagreement with the experimental data and our results is found, it will be necessary to validate our computational model, for example, on how to correct for the effective Coulomb interaction U. From this, we could improve the present computational methods and obtain a better prediction on optimum reactive gas combinations for an effective RIE process.

4. Summary

The optimum gas combinations for the reactive ion etching (RIE) processes on the CoO(001) surface has been studied using first principles calculations with the LDA and LDA + U methods. For the most favorable reaction process, the reactive gas should contain CH_4, and $Co_2(CO)_8$ could be one of most favorable by-products. Moreover, combining N_2 with other reactive gases hinders the etching process for the CoO surface. By applying the LDA + U method, although total energy values differed in the different states, the same optimum gas combinations and reaction products were obtained as with the LDA approach.

Acknowledgments

This work is partly supported by the Ministry of Education, Culture, Sports, Science and Technology of Japan (MEXT), through their Special Coordination Funds for the global Center of Excellence (COE) program (H08) 'Center of Excellence for Atomically Controlled Fabrication Technology' and the New Energy and Industrial Technology Development Organization (NEDO). Some of the calculations presented here were performed using the computer facilities of Cyber Media Center (Osaka University), the Institute of Solid State Physics (ISSP) Super Computer Center (University of Tokyo), the Yukawa Institute (Kyoto University), and the Japan Atomic Energy Agency (JAEA).

References

[1] Chae H, Vitale S A and Sawin H 2003 *J. Vac. Sci. Technol.* A **21** 381
[2] Alves Marco A R, Porto Lésnir F, de Faria Pedro H L and Braga Edmundo S 2004 *Vacuum* **72** 485
[3] Knizikevičius R 2006 *Vacuum* **81** 230
[4] Sahafi H F, Goldspink G F, Webb A P and Carter M A 1993 *Vacuum* **44** 263
[5] Villalvilla J M, Santos C and Vallés-Abarca J A 1994 *Vacuum* **45** 1113
[6] Takano F, Shima H, Kokaze Y, Nishioka Y, Suu K, David M, Roman T, Kasai H and Akinaga H 2007 *Proc. 24th Plasma Processing Workshop (Osaka)*
[7] Shima H, Takano F, Akinaga H, Tamai Y, Inoue I H and Takagi H 2007 *Appl. Phys. Lett.* **91** 012901
[8] Sanchez M J, Inoue I H and Rozenberg M J 2007 *Appl. Phys. Lett.* **91** 252101
[9] Shima H, Takano F, Muramatsu H, Yamazaki M, Akinaga H and Kogure A 2008 *Phys. Status Solidi (RRL)* **2** 99
[10] Inoue I H, Yasuda S, Akinaga H and Takagi H 2008 *Phys. Rev.* B **77** 35105
[11] Watanabe S, Diño W A, Nakanishi H, Kasai H and Akinaga H 2005 *Japan. J. Appl. Phys.* **44** 893
[12] David M, Muhida R, Roman T, Kunikata S, Dino W A T, Nakanishi H, Kasai H, Takano F, Shima H and Akinaga H 2007 *J. Phys.: Condens. Matter* **19** 365210
[13] Kishi H, Ozawa N, David M, Roman T, Nelson A, Dino W, Nakanishi H, Kasai H, Takano F, Shima H and Akinaga H 2008 *J. Vac. Soc. Japan* **51** 63
[14] David M, Muhida R, Roman T, Nakanishi H, Dino W, Kasai H, Takano F, Shima H and Akinaga H 2008 *Vacuum* at press
[15] Wang L, Maxisch T and Ceder G 2006 *Phys. Rev.* B **73** 195107
[16] Calzado C J, Hernández N C and Sanz Fdez J 2008 *Phys. Rev.* B **74** 045118
[17] Anisimov V I, Zaanen J and Andersen O K 1991 *Phys. Rev.* B **44** 943
[18] Dudarev S L, Botton G A, Savrasov S Y, Humphreys C J and Sutton A P 1998 *Phys. Rev.* B **57** 1505
[19] Kresse G and Joubert D 1999 *Phys. Rev.* B **59** 1758
[20] Kresse G and Furthmüller J 1996 *Phys. Rev.* B **54** 11169
[21] Bredow T and Gerson A R 2000 *Phys. Rev.* B **61** 5194
[22] Roth W L 1958 *Phys. Rev.* **110** 1333
[23] Zimmermann R, Steiner P, Claessen R, Reinert F, Hufner S, Blaha P and Dufek P 1999 *J. Phys.: Condens. Matter* **11** 1657
[24] Dartnell N J, Flowers M C, Greef R, Zhu J and Blackbur A 1995 *Vacuum* **46** 349